Electronic Supplementary Information

Superparamagnetic iron-doped nanocrystalline apatite as delivery system for doxorubicin

Michele Iafisco[†*], Christophe Drouet[‡*], Alessio Adamiano[†], Patricia Pascaud[‡§], Monica Montesi[†], Silvia Panseri[†], Stephanie Sarda[‡] and Anna Tampieri[†]

[†]Institute of Science and Technology for Ceramics (ISTEC), National Research Council (CNR), Via Granarolo 64, 48018 Faenza, Italy

[‡]CIRIMAT Carnot Institute, University of Toulouse, UMR CNRS/INPT/UPS 5085, Ensiacet, 4 allée Emile Monso, 31030 Toulouse cedex 4, France

[§]Present address: University of Limoges, CNRS, SPCTS UMR 7315, CEC, 12 Rue Atlantis, 87068 Limoges Cedex, France

Author for correspondence: Dr. Michele Iafisco
                                     E-mail: michele.iafisco@istec.cnr.it
                                     Tel: +39 0546699730
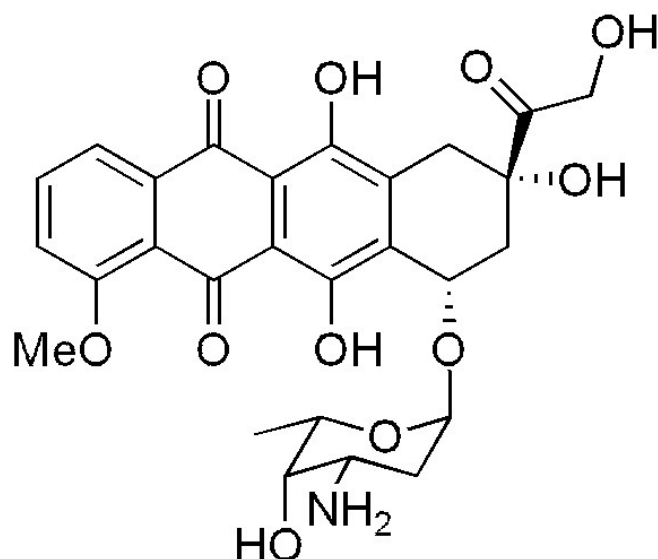
                                     Dr. Christophe Drouet
                                     E-mail: christophe.drouet@ensiacet.fr
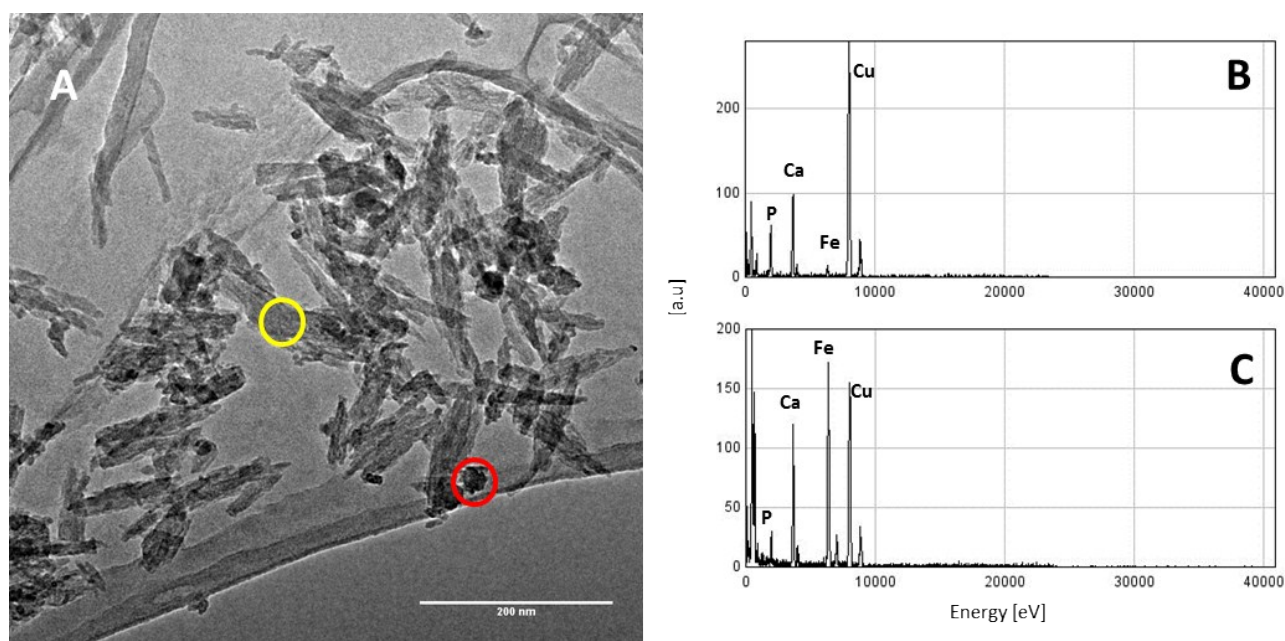   Tel: +33 0534323411

Figure S1. Pictures of the home-made device for the experiments in presence of pulsed electromagnetic fields (PEMF).

**Figure S2.** Molecular structure of doxorubicin (DOX)

Figure S3. (A) TEM image of FeHA. The areas marked with the red and yellow circles represent parts of the sample containing and not containing dark spots, respectively. EDX microanalyses of the areas of panel A marked with (B) yellow and (C) red circle.
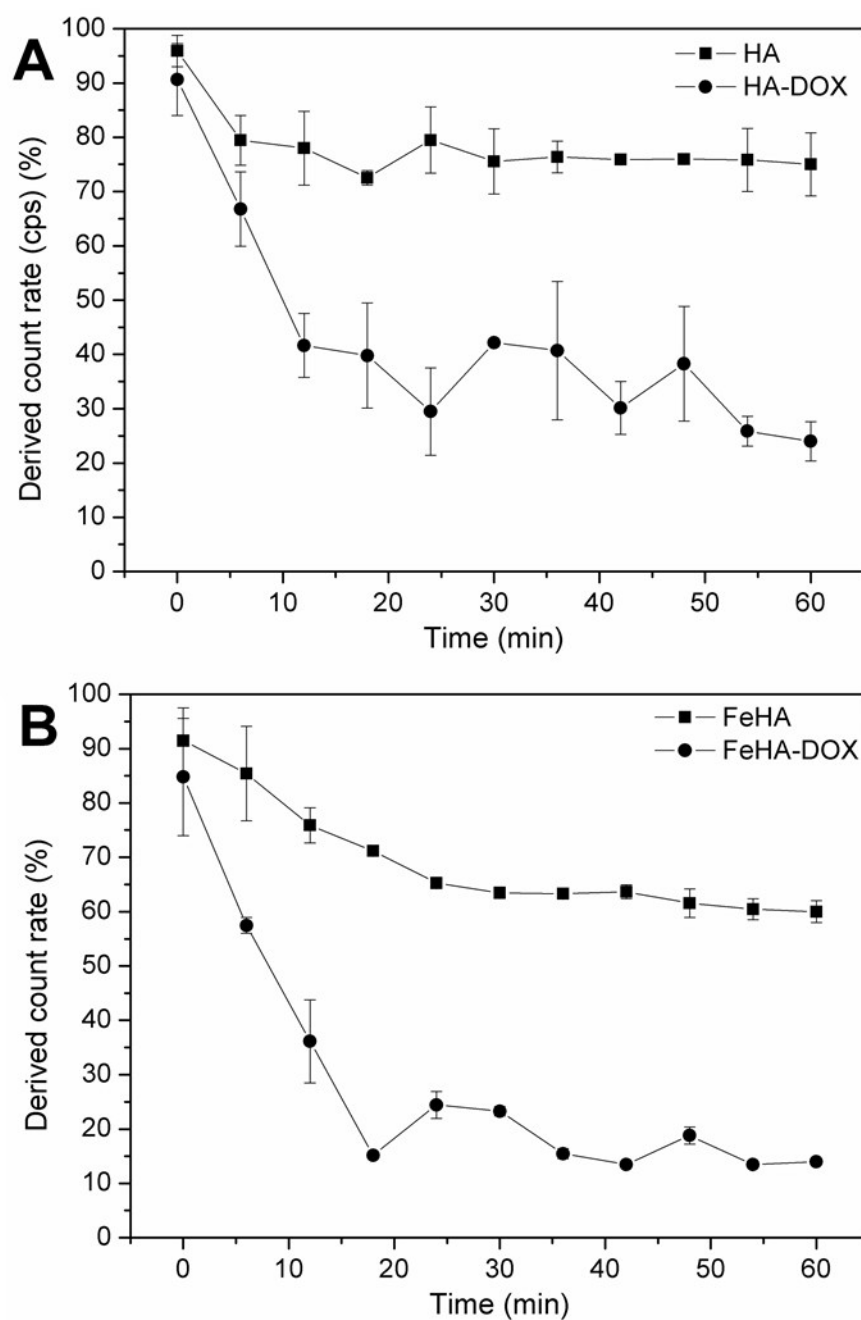
Figure S4. Percentage of derived count rate (cps) as a function of time (60 min) analyzed by DLS for (A) HA and HA-DOX and (B) FeHA and FeHA-DOX (0.1 mg mL^{-1}) in 0.01 M HEPES buffer at pH 7.4 and 25°C.
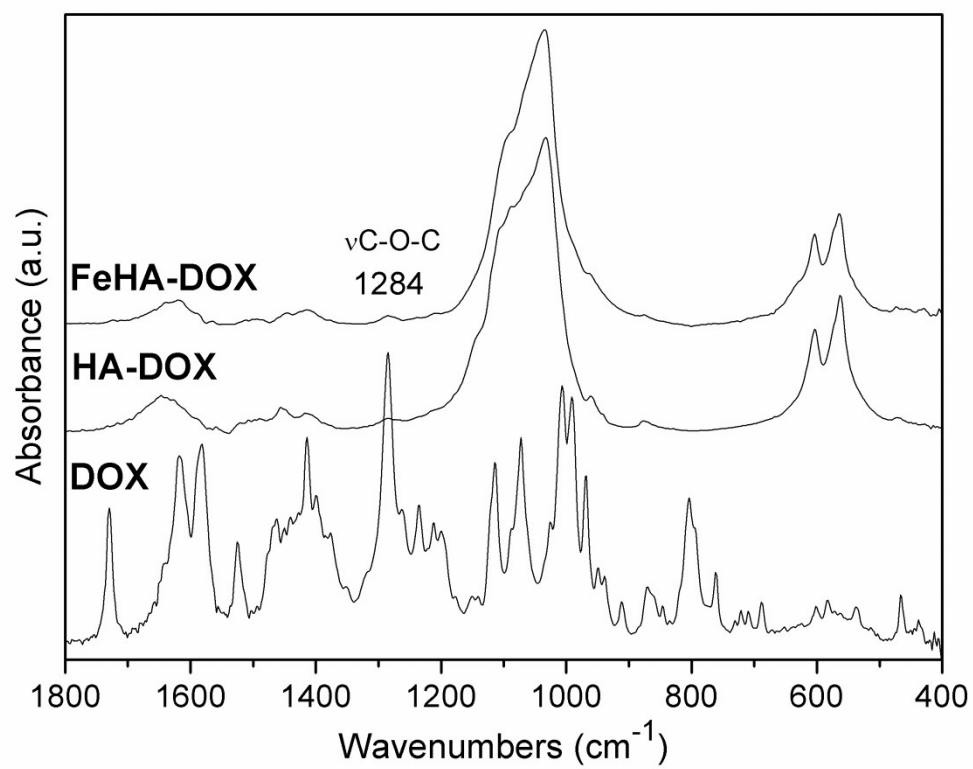
**Figure S5**. FTIR spectra of free DOX, HA-DOX and FeHA-DOX
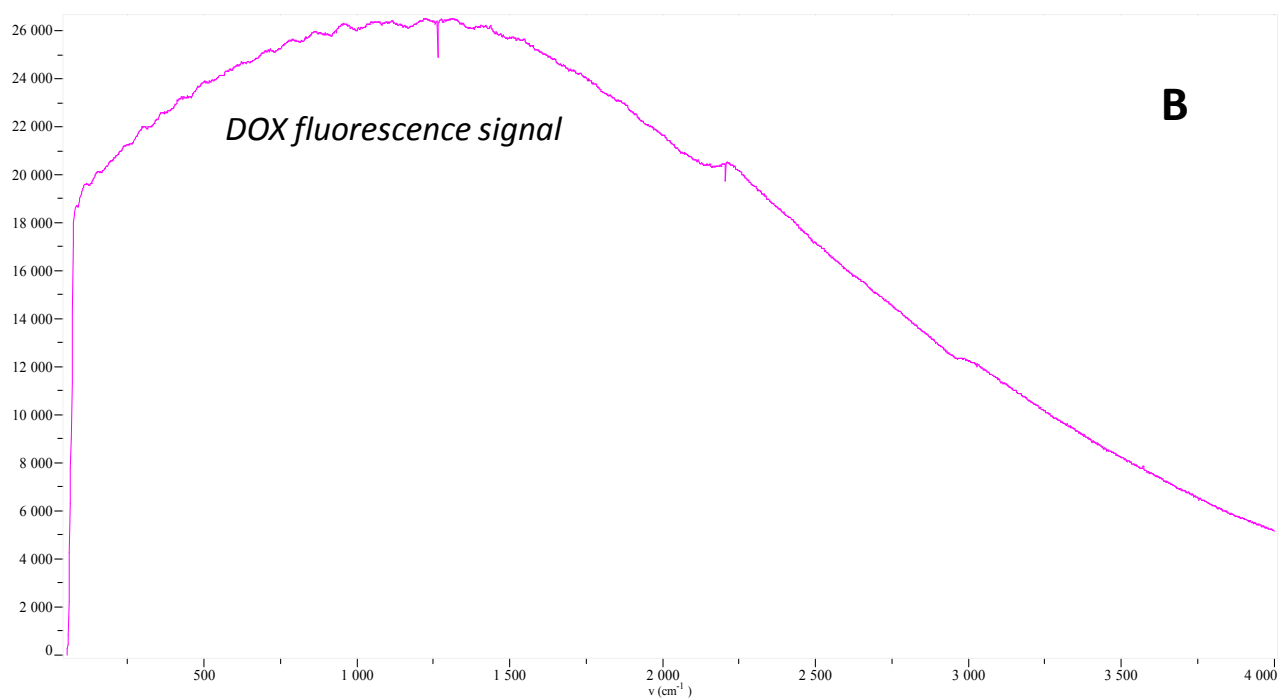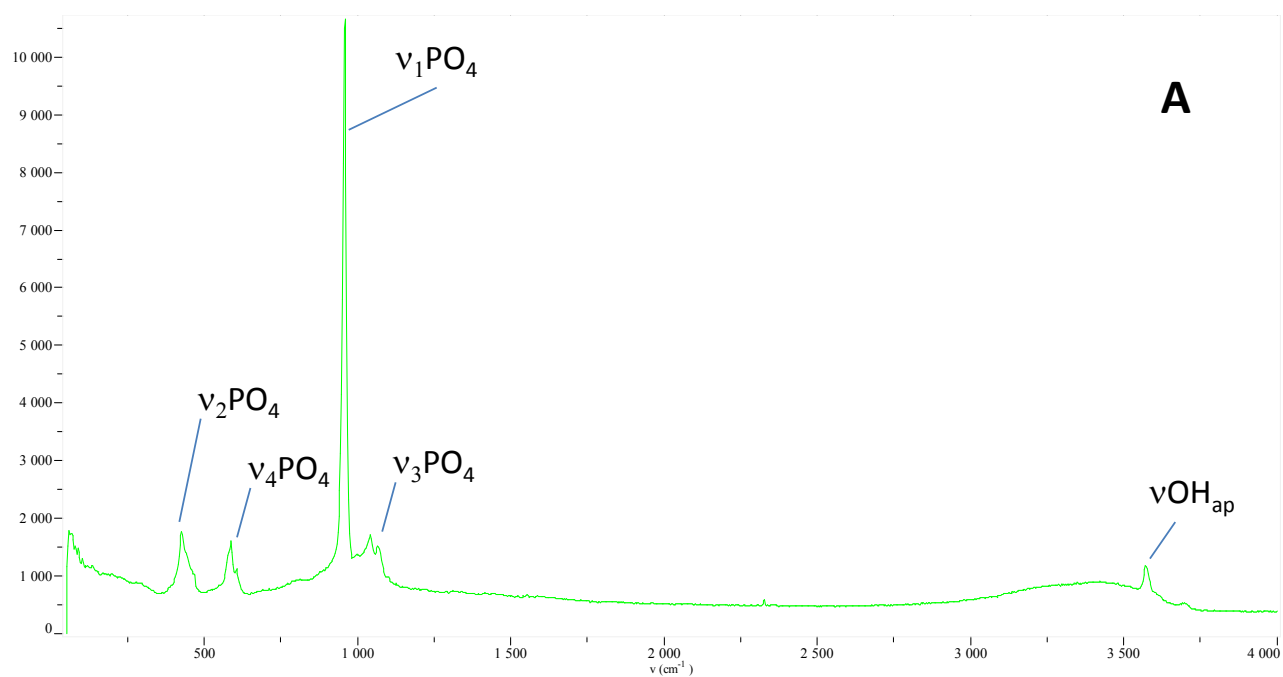
Figure S6. Raman spectra (laser wavelength 633 nm) for HA substrate (A) and DOX-HA (B). The presence of DOX leads to a broad fluorescence halo preventing direct observation of DOX/apatite interactions.
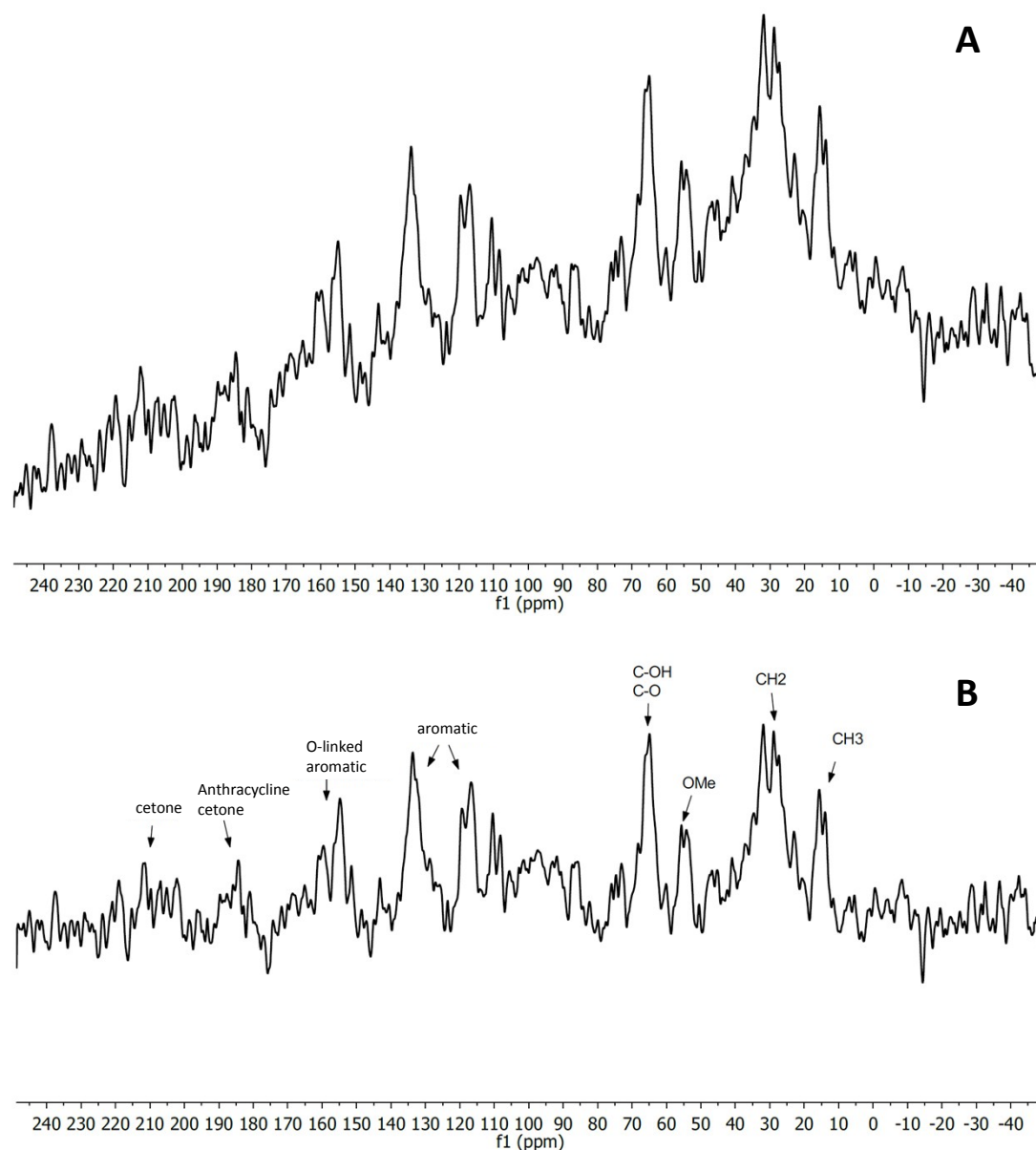
Figure S7. ^{13}C CP/MAS NMR spectra for DOX-HA before (A) and after (B) baseline correction. The noisy background does not allow clear determinations of peak positions so as to explore DOX/apatite interactions.
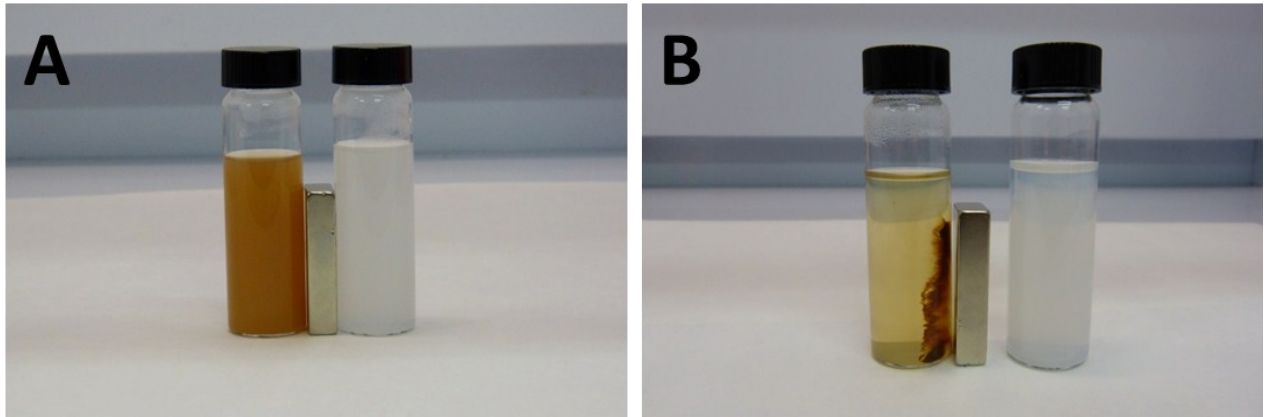
Figure S8. Pictures of FeHA (brown) and HA (white) water suspensions in contact with static magnetic field of 320 mT at different times (i.e. (A) immediately and (B) after 2 hours).
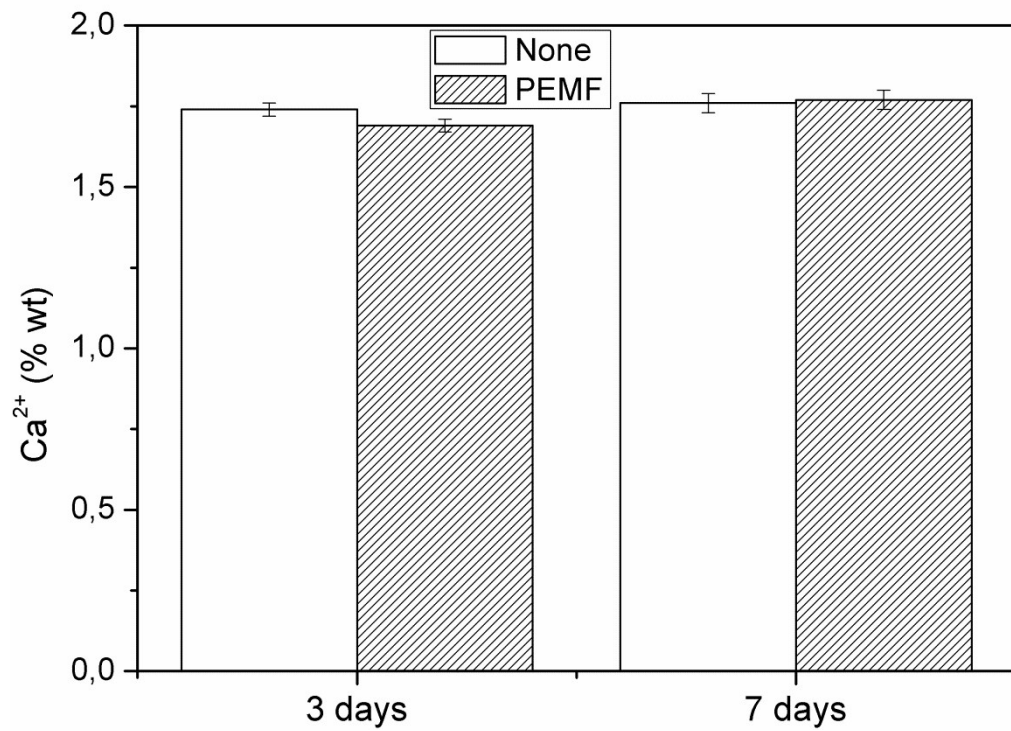
Figure S9. Weight percentage (calculated respect to initial amount of Ca^{2+}) of Ca^{2+} released from FeHA without (None) and in presence of pulsed electromagnetic fields (PEMF).

Table S1. Samples identification. Labelling of the samples, amount of DOX (µg of DOX on mg of NPs) loaded onto HA and FeHA and concentration (µg/ml) of the samples tested for the cellular study.

Samples	DOX loaded on NPs (µg/mg)	DOX (µg/ml)	NPs (µg/ml)
HA-DOX 100µM	475	54	114.3
HA Ct_1	-	-	114.3
HA-DOX 10µM	475	5.4	11.43
HA Ct_2	-	-	11.43
FeHA-DOX 100µM	449	54	120.5
FeHA Ct_1	-	-	120.5
FeHA-DOX 10µM	449	5.4	12.05
FeHA Ct_2	-	-	12.05
DOX 100µM	-	54	-
DOX 10µM	-	5.4	-

Table S2. Correlation coefficients (R^2) for mathematical fits of DOX release kinetic data (from HA and FeHA and in presence and in absence of PEMF) with regard to several models

Kinetic release models	HA without PEMF	HA with PEMF	FeHA without PEMF	FeHA with PEMF
Zero order model	0.930	0.817	0.737	0.922
First order model	0.777	0.681	0.691	0.844
Gas -like desorption model	0.636	0.642	0.718	0.003
Higuchi (particular case of KP) model	0.981	0.904	0.840	0.941
Korsmeyer-Peppas (KP) model	0.952	0.892	0.900	0.933
Hixson-Crowell (HC) model	0.835	0.727	0.707	0.873

	HA without PEMF	HA with PEMF	FeHA without PEMF	FeHA with PEMF
exponential diffusion factor in KP model	0.69	0.52	(0.29)	0.86
standard deviation	0.11	0.14	0.08	0.20